





Information theoretic measures for interacting bosons in optical lattice

Rhombik Roy ¹, Barnali Chakrabarti,¹ N. D. Chavda ², and M. L. Lekala ³

¹*Department of Physics, Presidency University, 86/1 College Street, Kolkata 700073, India*

²*Department of Applied Physics, Faculty of Technology and Engineering,
The Maharaja Sayajirao University of Baroda, Vadodara-390001, India*

³*Department of Physics, University of South Africa, P.O. Box 392, Pretoria 0003, South Africa*

 (Received 30 May 2022; revised 13 December 2022; accepted 19 January 2023; published 13 February 2023)

This work reports the different information theoretic measures, i.e., Shannon information entropy, order, disorder, complexity, and their dynamical measure for the interacting bosons in an optical lattice with both commensurate and incommensurate filling factor. We solve the many-body Schrödinger equation from first principles by multiconfigurational time-dependent Hartree method which calculates all the measures with high level of accuracy. We find for both relaxed state as well as quenched state the López-Ruiz–Mancini–Calbet (LMC) measure of complexity is the most efficient depicter of superfluid (SF) to Mott-insulator transition. In the quench dynamics, the distinct structure of LMC complexity can be used as a “figure of merit” to obtain the timescale of SF to Mott state entry, Mott holding time, and the Mott state to SF state entry in the successive cycles. We also find that fluctuations in the dynamics of LMC complexity measure for incommensurate filling clearly establish that superfluid to Mott-insulator transition is incomplete. We overall conclude that distinct structure in the complexity makes it more sensitive than the standard use of Shannon information entropy.

DOI: [10.1103/PhysRevE.107.024119](https://doi.org/10.1103/PhysRevE.107.024119)

I. INTRODUCTION

In the recent years, different information theoretic measures have been proposed in several scientific disciplines. It has been established that the information theoretical measures are the most conceptual tool for the study of structures in various kinds of systems [1–9]. Out of these, entropic uncertainty relations, order, disorder, and complexity in quantum mechanical systems become the trademark [10–14]. In this context, the concept of complexity has attracted considerable interest [15–22]. Measure of complexity is utilized to characterize how a physical or biological system will organize itself in response to a change in the external parameters. It is usually believed that, with increase in number of particles N , the complexity would also increase. Although there are several definitions of complexity in the literature [23–26], the usual definition of complexity $\Gamma_{\alpha\beta}$ was introduced by Shiner, Davison, and Landsberg [27], known as SDL complexity. The other statistical measure of complexity C was defined by López-Ruiz, Mancini, and Calbet [24,28] and known as LMC measure. In the context of measuring Shannon information entropy, complexity is taken as the most efficient measure of how much order and disorder exist in a system [29–35]. The most common case is the “convex” type complexity where it is minimum both for completely ordered and disordered systems. Some systems also exhibit complexity which is either increasing or decreasing functions of disorder [27]. The concept of statistical complexity was first successfully applied in atomic system by the group of Panos [15]. Both SDL and LMC were studied as a function of atomic number Z and their main interest was to explore the connection of the periodicity of shell structure with the complexity measures. In a recent

work, LMC complexity measure is presented as an efficient detector for the study of lowest bound and unbound electronic states of diatomic molecule [9].

In this work, we are interested in the SDL and LMC complexity measures for interacting bosons in the optical lattice. The realization of fully controlled quantum many-body systems has been an outstanding challenge in recent years. Interacting bosons in an external trap at ultracold temperature allow unprecedented experimental control and serve as the ideal test bed to study quantum many-body physics. It features several quantum phases: superfluid phase (SF), Mott-insulator phase (MI), and fragmented Mott insulator (FMI) [36]. In the pioneering experiment of Greiner *et al.* [37], a quantum phase transition is observed in a Bose-Einstein condensate (BEC) kept in an optical lattice potential with repulsive interatomic interaction. It is observed that weakly interacting bosons in shallow optical lattice exhibit a superfluid phase. In the SF phase, the atoms exhibit long-range phase coherence across the lattice. By gradual increase in the depth of the lattice, SF phase makes a transition to Mott-insulator phase. In MI phase, atoms are localized in the individual lattice sites, and phase coherence across the lattice is lost. The quantum phases are studied by Bose-Hubbard model [38,39], *ab initio* many-body technique, and multiconfigurational time-dependent Hartree for bosons (MCTDHB) [36,40–42]. The many-body features are characterized by distinct measures of many-body correlation, collapse, and revival dynamics in lattice depth quench [43]. The collapse-revival dynamics in the measure of correlation show the exact behavior of Fig. 2 of Ref. [44].

In this work, we like to follow the pathway from SF phase to the insulating phase by directly monitoring the change in order, disorder, and complexity. Our main attention is to

explore the crossover from SF phase to MI phase through the nonmonotonic dependence of LMC complexity on the lattice depth parameter. We present a systematic study to establish that lattice depth parameter can be taken as a parameter of order and disorder. We observe a *distinct* maxima in the LMC measure of complexity when a system of interacting bosons smoothly passes from SF phase to MI phase. We establish that LMC complexity is a sensitive descriptor and more rich measure than entropy to study the pathway from SF to MI phase. In quench dynamics, LMC measure establishes how the system becomes self-organized in sudden increase of lattice depth. We also find that LMC complexity measure is a richer quantity compared to Shannon information entropy (SIE) even for quench dynamics. During the quench process, when the system passes through successive cycles of SF to MI phase (Greiner's experiment [44]), the most important measure is the timescale. We find entropy fails to detect the different timescale due to its monotonic oscillating behavior. Whereas the distinct structure in complexity dynamics establishes that LMC complexity is a more featured measure and can be taken as a "figure of merit" to find the timescale with high precision.

We consider a system of $N = 3$ bosons interacting with a contact interaction $\hat{W}(x_i - x_j) = \lambda\delta(x_i - x_j)$ in one-dimensional three-well optical lattice, λ is the strength of interaction, and the bosons are trapped in a lattice of the form $V_{\text{OL}}(x) = V_0\sin^2(kx)$, where V_0 is the depth of the optical lattice and k is the periodicity of the lattice. Lattice depth is experimentally tunable. In this work, lattice depth is tuned to achieve SF phase to MI phase transition. We solve the many-body Schrödinger equation at a high level of accuracy by MCTDHB method (presented in Sec. II).

The general information theoretical measure includes Shannon information entropy measures, order (Ω), disorder (Δ), and complexity (given in Sec. III), we calculate SDL complexity $\Gamma_{\alpha\beta} = \Delta^\alpha\Omega^\beta$ for several values of α and β . We observe that the lattice depth parameter acts as a measure of order-disorder and complexity shows all the three types of behavior as defined in literature [27] depending on the choice of α and β . The most interesting is $\Gamma_{1,1}$ which exhibits convex type nature. We also note that the SF phase is characterized by maximum order and the MI phase exhibits maximum disorder. The "SF-MI" transition can be termed as "order-disorder" transition in the language of statistical measures.

Although the SDL measure of complexity is a powerful tool to identify the type of complexity inherent in a complex many-body system, it is uniquely determined by the disorder (Δ) of the system. It is reasonable to say that the complexity cannot be solely defined by the measure of entropy and system size. Although $\Gamma_{1,1}$ seems to be an efficient measure of complexity, it requires further investigation. Here we measure the LMC complexity as it is more deterministic and not as overuniversal as SDL measure. In this paper, we numerically calculate both LMC and SDL complexity as a function of the lattice depth parameter following the procedure mentioned in Sec. III. Our goal is to find out the best value of (α, β) for which $C \simeq \Gamma_{\alpha\beta}$. We choose the pair of $(\alpha, \beta) = (\frac{1}{4}, 0), (1, 1),$ and $(0, 4)$. In all cases, we observe different trends of $\Gamma_{\alpha\beta}$, i.e., increasing or decreasing, or convex type. However, we find

a significant overall similarity between $\Gamma_{1,1}$ and C . For other choices of (α, β) , we observe less similarity.

We also establish that out of all information theoretic measures, complexity is the most sensitive measure. With increase in lattice depth, when the system smoothly passes from SF phase to MI phase, the corresponding information entropy smoothly increases with no clear signature at what value of lattice depth the crossing happens. We find the complexity measure clearly shows a distinct maxima at the point of crossing and we conclude complexity is a richer and more sensitive measure than the entropy.

For lattice depth quench, we prepare an initial state, which is a pure SF phase. An instantaneous increase in the lattice depth triggers the system to go into the MI phase. From the time evolution of entropy measures, we further calculate the time dynamics of complexity. We observe collapse revival in short time dynamics, as discussed in detail in Sec. IV. We again observe that maximum order is associated with SF phase and MI phase is associated with maximum disorder. However, the intriguing observation is that we are able to focus on the timescale of entry and exit of different phases over several cycles. We find the holding time of the Mott phase, which is exposed as a plateau region in the time dynamics of complexity. Although the corresponding entropy demonstrates the collapse revival cycle, however, its nondistinct behavior can not find the timescale of different cycles. This observation reconfirms that complexity dynamics is a more sensitive descriptor than the time evolution of entropy.

The intriguing physics is also observed when the filling factor $\nu = \frac{N}{W}$ is not equal to unity. In this article, we have studied the distinct case of $\nu < 1$, where the true Mott phase is never possible. Entropy again exhibits the oscillatory behavior as before which should signify the SF-MI collapse revival cycle [43]. Thus, it is more confusing and may lead to a wrong conclusion as for $\nu < 1$, SF to true MI transition does not happen. However, the corresponding complexity exhibits fluctuation and the plateau region disappears. It clearly manifests that SF to MI transition is incomplete. We reconfirm that complexity is the best deterministic measure to depict the SF-MI transition and the corresponding timescale. We also find that in the collapse-revival dynamics, the system does not return to the initial SF phase in long time.

The paper is structured as follows. In Sec. II, we introduce the setup and the necessary theory. Section III deals with the basic equations to measure the different quantities. Section IV explains our numerical results. Section V draws our conclusions.

II. SETUP AND METHODOLOGY

In this work, we consider $N = 3$ bosons confined in one-dimensional (1D) optical lattice and interacting with contact interparticle interaction. This one-dimensional regime is easily achieved by tight transverse confinement. Quantum many-body effect is also important in such reduced dimension as the quantum fluctuation plays an important role. The Hamiltonian for N interacting bosons in 1D optical lattice is

given by

$$H = \sum_{i=1}^N \left(-\frac{1}{2} \frac{\partial^2}{\partial x^2} + V_{\text{OL}}(x_i) \right) + \sum_{i<j} \hat{W}(x_i - x_j), \quad (1)$$

where V_{OL} represents the external lattice potential and $\hat{W}(x_i - x_j)$ is the two-body interaction. We make the Hamiltonian dimensionless by dividing it by the factor $\frac{\hbar^2}{mL^2}$, where m is the mass of the bosons and L is some arbitrary length scale. The Hamiltonian is scaled in terms of recoil energy $E_R = \frac{\hbar^2 k^2}{2m}$. Thus, the time is expressed in units of $\frac{\hbar}{E_R}$ and the unit of distance becomes k^{-1} . We use natural units, i.e., $\hbar = m = k = 1$. We fix up the grid at $x_{\min} = -\frac{3\pi}{2}$ to $x_{\max} = \frac{3\pi}{2}$ which can accommodate three wells. We find the stationary solution of the many-body Schrödinger equation by MCTDHB implemented in the MCTDH-X software [45–47] with periodic boundary condition. In MCTDHB, the wave function of the interacting bosons is expanded over a set of permanents which are the symmetrized bosonic states of N bosons distributed over M single particle states:

$$|\Psi(t)\rangle = \sum_{\vec{n}} C_{\vec{n}}(t) |\vec{n}; t\rangle. \quad (2)$$

The vector $\vec{n} = (n_1, n_2, \dots, n_M)$ represents the occupation of the orbitals and $n_1 + n_2 + \dots + n_M = N$ preserve the total number of particles:

$$|\vec{n}; t\rangle = \prod_{i=1}^M \left(\frac{(b_i^\dagger(t))^{n_i}}{\sqrt{n_i!}} \right) |\text{vac}\rangle. \quad (3)$$

$b_k^\dagger(t)$ creates a boson occupying the time-dependent orbital $\phi_k(x, t)$. The number of possible configurations are $\binom{N+M-1}{N}$. It is important to note that both the expansion coefficients $[C_{\vec{n}}(t)]$ and the orbitals $[\phi_i(x, t)]$ that build the permanents $|\vec{n}, t\rangle$ are time dependent and fully variationally optimized quantities. Thus, MCTDHB has been established as the most efficient way to solve the time-dependent many-body Schrödinger equation [48–50]. The efficiency of MCTDHB is to make the sampled Hilbert space dynamically follow the time evolution of the many-body system. MCTDHB has been widely used in different theoretical calculations [36,51–53] and results are very close to experimental predictions [54,55]. For $M \rightarrow \infty$ limit, as the set of permanents $|\vec{n}; t\rangle$ span the complete Hilbert space, the expansion is exact. But during computation, we limit the size of the Hilbert space. As the permanents are now time dependent, a given degree of accuracy is achieved with the truncated basis as compared to a time-independent basis. It is also proved that significant computational advantage is achieved over exact diagonalization [56]. To solve the time-dependent many-body Schrödinger equation $\hat{H}|\psi\rangle = i\frac{\partial|\psi\rangle}{\partial t}$ for the wave function $|\psi\rangle$, we calculate the time evolution of the coefficients $C_{\vec{n}}(t)$ and the orbitals $\phi_i(x, t)$. We utilize variational principle [57–60] to obtain the equation of motion of the time-dependent coefficient and orbital [48,49,61–63]. Finally, the coupled nonlinear integrodifferential equations (IDE) are solved by MCTDHB package [47]. For the calculation of the eigenstates of the Hamiltonian, we propagate the MCTDHB equations in imaginary time,

called improved relaxation method. For quench dynamics, we consider the total Hamiltonian

$$\hat{H}(x_1, x_2, \dots, x_N) = \sum_{i=1}^N \hat{h}(x_i) + \Theta(t) \sum_{i<j=1}^N \hat{W}(x_i - x_j), \quad (4)$$

where $\hat{h}(x)$ is the one-body part that includes the external trap and kinetic energy. $\Theta(t)$ is the Heaviside step function of time t which triggers the quench at $t = 0$.

III. MEASURES OF ORDER-DISORDER, COMPLEXITY, AND CORRELATION

The key quantity for the calculation of order and disorder is entropy S . Shannon information entropies, both in coordinate space and momentum space, are usually taken as the key measure of information entropy. They are defined as $S_x(t) = -\int dx \rho(x, t) \ln[\rho(x, t)]$ and $S_k(t) = -\int dk \rho(k, t) \ln[\rho(k, t)]$, where $\rho(x, t)$ is the one-body density in position space and $\rho(k, t)$ is the same in momentum space. The reduced one-body density in coordinate space is defined as

$$\rho^{(1)}(x'_1|x_1; t) = N \int dx_2 dx_3 \dots dx_N \psi^*(x'_1, x_2, \dots, x_N; t) \times \psi(x_1, x_2, \dots, x_N; t). \quad (5)$$

Its diagonal gives the one-body density $\rho(x, t)$ defined as

$$\rho(x; t) = \rho^{(1)}(x'_1 = x|x_1 = x; t). \quad (6)$$

Density distributions are normalized to unity. However, the one-body density is insensitive to address correlations present in the many-body wave function. So we define an alternative measure of many-body information entropy as

$$S = -\sum_i \bar{n}_i(t) \ln \bar{n}_i(t), \quad (7)$$

where $\bar{n}_i(t) = \frac{n_i(t)}{N}$ are the eigenvalues of the reduced one-body density matrix. This can be called occupational information entropy. For the mean-field theory as there is only one natural occupation, occupational entropy is always zero. In our earlier calculation [43], we have also discussed how time evolution of occupational entropy can be chosen as a good measure for the description of fragmentation. It is also a key quantity in the study of nonequilibrium quench dynamics to establish whether thermalization and relaxation are ubiquitous in nature.

A. SDL measure of complexity

Complexity is measured in terms of order and disorder. Often, entropy was taken as an appropriate measure of disorder. However, with increase in the number of available states, the disorder of the system increases, as well as entropy increases. Later, Landsberg's definition of the disorder parameter (Δ) is well accepted, which circumvents the previous problem. Disorder is defined as

$$\Delta = \frac{S}{S_{\max}}, \quad (8)$$

where S is the actual information entropy of the system. S_{\max} is the maximum entropy which is accessible to the system.

Thus, in the Landsberg definition, entropy and disorder are decoupled. Order is defined as

$$\Omega = (1 - \Delta). \quad (9)$$

$\Omega = 1$ corresponds to perfectly ordered and predictable system. $\Omega = 0$ corresponds to complete disorder and randomness. Both order and disorder are size independent and lie between 0 and 1. The measure of complexity is further defined appropriately in terms of order and disorder. In the literature, we find three categories of complexity measure, as mentioned in the Introduction. To take into account all three categories, we utilize the most generic form of complexity, defined as

$$\Gamma_{\alpha\beta} = \Delta^\alpha \Omega^\beta = \Delta^\alpha (1 - \Delta)^\beta = (1 - \Omega)^\alpha \Omega^\beta. \quad (10)$$

It defines the complexity of disorder strength α and order strength β . Thus, three categories are subsumed here. With $\beta = 0$ and $\alpha > 0$, complexity is an increasing function of disorder; with $\alpha = 0$ and $\beta > 0$, complexity is an increasing function of order. When $\alpha \neq 0$, $\beta \neq 0$, one finds the most common case of convex type complexity. Complexity vanishes at zero disorder and zero order and exhibits a maximum in-between.

B. LMC measure of complexity

The most interesting is the behavior of $\Gamma_{1,1}$ in the measure of SDL complexity. Although it can be considered a useful structural measure of complexity, but $\Gamma_{1,1}$ measure is criticized as ‘‘overuniversal’’ by Feldman and Crutchfield [64], as it is uniquely determined by disorder (Δ). Thus, this criticism is applicable for any other measure of complexity as well, i.e., for any values of α and β . Here we consider another statistical measure of complexity. The LMC measure is defined as

$$C = SD, \quad (11)$$

where S denotes the information content stored in the system. In our calculation, $S = S_x + S_k$. Total information of the system is defined as the sum of Shannon information entropy in coordinate space (S_x) and Shannon information entropy in momentum space (S_k). D corresponds to the disequilibrium of the system. For continuous probability distribution in position space as well as momentum space

$$D = D_x D_k, \quad (12)$$

where

$$D_x = \int \rho^2(x) dx \quad (13)$$

and

$$D_k = \int \rho^2(k) dk. \quad (14)$$

So, we numerically calculate the LMC measure of complexity by $C = SD$ and the SDL measure of complexity by $\Gamma_{\alpha\beta} = \Delta^\alpha \Omega^\beta$ as a function of lattice depth parameter V_0 .

C. Measure of correlation

A superfluid phase exhibits global correlation across the lattice whereas the Mott phase exhibits onsite correlations. To explore the link between order-disorder to complexity, we

further make an analysis of first-order correlation function $g^{(1)}(x', x, t)$, defined as

$$g^{(1)}(x', x; t) = \frac{\rho^{(1)}(x'|x; t)}{\sqrt{\rho(x, t)\rho(x', t)}}, \quad (15)$$

where $\rho^{(1)}(x'|x; t)$ is the one-body reduced density matrix and $\rho(x, t)$ is the diagonal part of the one-body density matrix given in Eqs. (5) and (6). $g^{(1)}(x', x, t)$ quantify how the particles are correlated in the specific system. $g^{(1)}(x', x, t)$ is a good quantitative measure of first-order correlation [65,66]. In recent experiment with ultracold atoms in optical lattice, higher-order correlations are also measured experimentally [67–70]. Note that $g^{(1)}(x', x; t) < 1$ denotes a loss of coherence, which indicates that the visibility of interference fringes in the interference experiments will be less than 100%, whereas $g^{(1)}(x', x; t) = 1$ corresponds to full coherence, which implies the maximal fringe visibility in the interference pattern. Correlations are affected by the strength and nature of the interactions between the particles; for example, a larger loss of coherence occurs with a larger interparticle repulsion. It is to be noted that, similar to the normalized Glauber correlation function, one can utilize the quantum similarity index (QSI) [71]. Like $g^{(1)}(x', x; t)$, QSI also provides a real value range of [0,1] and has been successfully utilized in the measure of interelectronic correlation. However, in our present study, the use of $g^{(1)}(x', x; t)$ is more elegant.

IV. RESULTS

A. Measure of complexity in relaxed state

The present calculation is performed in one dimension with $N = 3$ repulsively interacting bosons in the optical lattice. The dimensionless strength parameter λ of the repulsive interaction is kept fixed to $\lambda = 0.3$ and the lattice depth potential is varied. We present detailed results for three particles in three wells, and in the Appendix, we briefly present results for seven particles in seven wells. For both calculations, we consider repulsive interaction and conclude that nature of complexity is independent of the size of the system.

As pointed out earlier, fragmentation is the hallmark of MCTDHB, where several natural orbitals exhibit significant population. Thus, convergence is an important issue, and to capture the correct physics, we need an adequate number of orbitals. For the stationary state solution, we follow the improved relaxation method: we propagate the MCTDHB equation in imaginary time. For relaxation, we keep $M = 6$ orbitals and find that with further increase in the number of orbitals, there is no change in the computed quantities. In Fig. 1, we plot the occupation of the first, second, and third natural orbitals as a function of lattice depth potential. For very small lattice depth, the first orbital has close to 100% occupation and second and third orbitals have insignificant occupation. The many-body wave function can be well approximated by the mean-field state $|N = 3, 0, 0, 0, 0, 0\rangle$. With increase in V_0 , fragmentation is built up and thus makes a transition from SF phase to fragmented phase. Finally, at $V_0 = 10.0$, we observe complete fragmentation with the occupation of first three natural orbitals by 33.33%. The corresponding

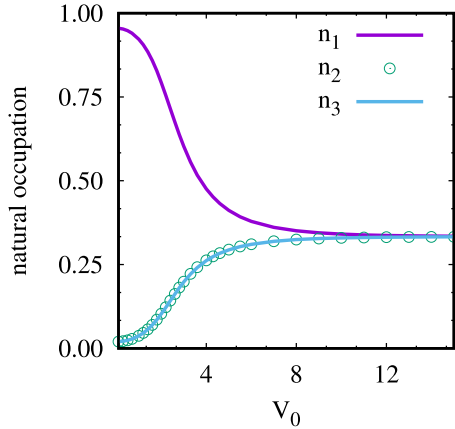


FIG. 1. Population of the first three natural orbitals as a function of lattice depth (V_0). As V_0 increases, the occupation in the first orbital starts to decrease while another two orbitals start to contribute. At $V_0 = 10.0$, the state becomes threefold fragmented ($n_1 \simeq n_2 \simeq n_3 \simeq \frac{1}{3}$).

configuration is $|1, 1, 1, 0, 0, 0\rangle$ which is a Mott state. Thus, for such a finite size system, there is a smooth crossover from SF phase to MI phase which is termed as *pathway*. The smooth crossover is nicely demonstrated by the gradual loss of global correlation across the lattice and finally keeping only the diagonal correlation with increase in V_0 . In Fig. 2, we plot the absolute value of the first-order correlation function $g^{(1)}(x', x, t)$. Figure 2(a) ($V_0 = 0.7$) exhibits both interwell and intrawell coherence which is a SF phase whereas Fig. 2(f) ($V_0 = 10.0$) exhibits only intrawell coherence with complete loss of interwell coherence which is a MI phase. It is clearly exhibited that between $V_0 = 2.5$ and 3.5 , the system exits SF phase and enters to fragmented phase. It is not possible to find out the exact value of V_0 when the crossover takes place which needs further study.

In Fig. 3(a), we plot the many-body SIE as a function of lattice depth (V_0). For SF phase, entropy is minimum but not zero. With increase in lattice depth, entropy gradually increases and finally saturates at $V_0 = 10.0$ which is the MI phase. With further increase in the lattice depth parameter, entropy remains at its saturation value. The monotonic increase in the entropy and its saturation detect the two phases; however, SIE is unable to find the crossover point.

In Fig. 3(b), We plot the order and disorder for varying lattice depth. We observe for SF state, order is maximum and disorder is minimum. As neither the order is one nor the disorder is zero, the SF state is not a *perfectly* ordered state. With increase in lattice depth, order gradually decreases and disorder increases. At $V_0 = 2.8$, order and disorder plots intersect each other, which we considered as the initiation of SF to MI state. At $V_0 = 10.0$, order becomes exactly zero and the disorder becomes exactly 1.0, which confirm that Mott phase is a *random* phase or a *perfectly* disordered phase. Thus, our numerical calculations exhibit that the ‘‘SF-MI’’ transition can be renamed as ‘‘order-disorder’’ transition. The corresponding SDL complexity $\Gamma_{\alpha\beta}$ is plotted in Fig. 3(c) for various choices of α and β . $\Gamma_{1,1}$ shows convex type, i.e., type II complexity. For SF phase, complexity is mini-

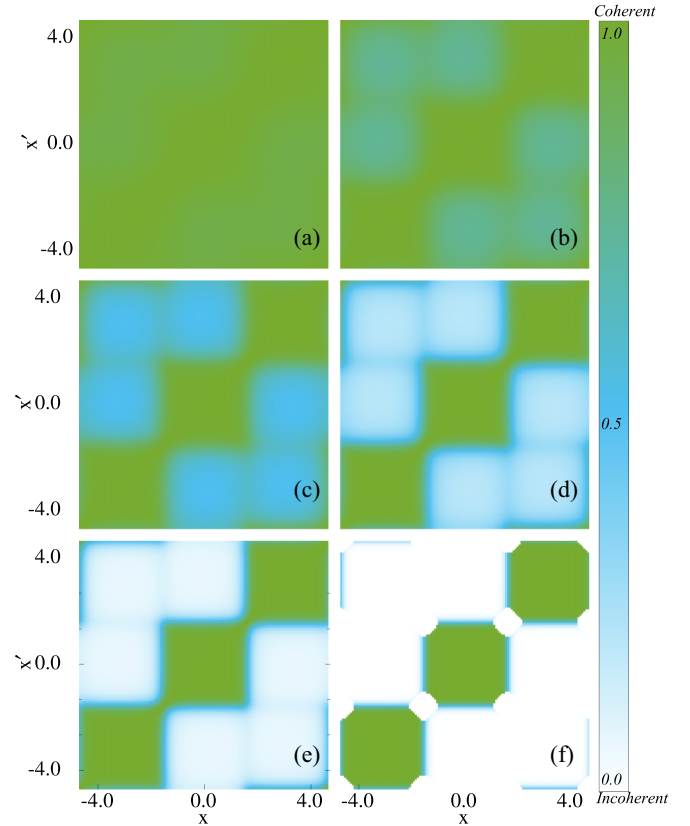


FIG. 2. First-order normalized correlation function $g^{(1)}(x', x, t)$ as a function of lattice depth (V_0). (a) $V_0 = 0.7$ is in the superfluid phase. A complete first-order coherence is observed within each well with $g^{(1)}(x', x, t) \simeq 1$; interwell coherence as well as intrawell coherence are maintained throughout the lattice. (b) $V_0 = 1.5$: it is a mixed state of SF and MI. Diagonal correlation starts to build up which means the loss of interwell coherence. (c) $V_0 = 2.5$: interwell coherence loss is now more prominent. (d) $V_0 = 3.5$: structure along the diagonal begins to emerge, while off-diagonal portions fade away. (e) $V_0 = 5.0$: MI is the dominating phase. Intrawell coherence is prominent whereas interwell coherence faded away. (f) $V_0 = 10.0$, $g^{(1)}(x', x, t) \simeq 1.0$ along the diagonal and $g^{(1)}(x', x, t) \simeq 0.0$ when $x \neq x'$, corresponds to pure MI phase at the cost of absolute loss of interwell coherence and 100% buildup of diagonal correlations.

um. With increase in lattice depth, complexity increases, reaches a maximum, and smoothly reduces to zero for Mott phase. Whereas for $\Gamma_{0,4}$, the complexity with zero disorder exhibits type III complexity of the literature [27]. $\Gamma_{1/4,0}$, the complexity with zero order, exhibits type I complexity [27]. Thus, we find the existence of all three types of complexity in our calculation. However, as in Fig. 3(c), we observe three different kinds of behavior in the measure of SDL complexity for different choices of α, β ; we fail to conclude which pair (α, β) values can uniquely define the nature of complexity. We found the definition given in Eq. (10) is overuniversal as complexity is basically determined by the disorder Δ for any arbitrary choice of α, β . So, we calculate a more informative measure of complexity C using the equations from Sec. III B. In Fig. 4, we plot LMC complexity C for different lattice depth parameter V_0 and observe C behaves similarly to $\Gamma_{\alpha\beta}$ only when $\alpha = 1$ and $\beta = 1$. It leads to conclude that the bosonic

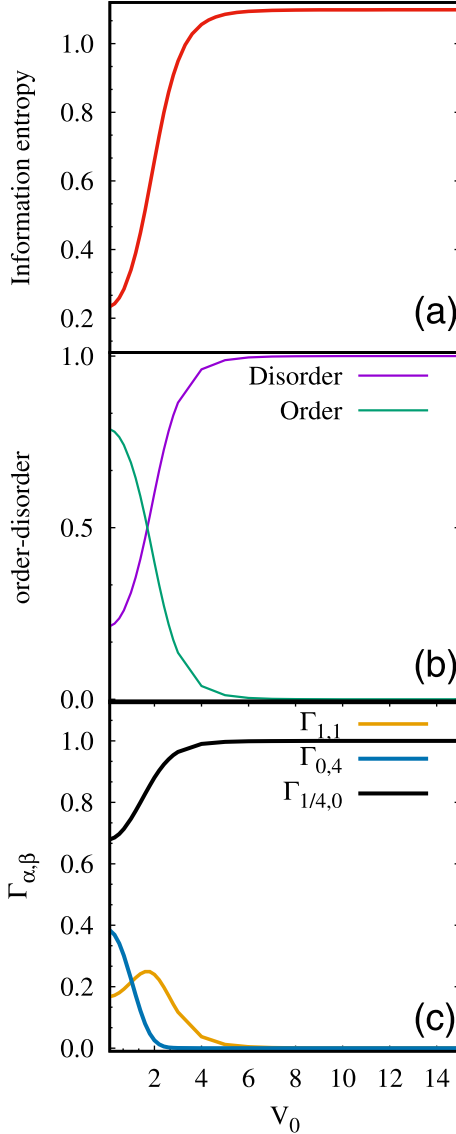


FIG. 3. (a) Plot of Shannon information entropy (S) as a function of lattice depth (V_0). Entropy is minimum for shallow lattice depth. As lattice depth increases, transition from SF to MI phase is followed by saturation in the entropy at maximum value. (b) Order and disorder: in the superfluid to Mott-insulator transition, order gradually decreases to zero and disorder gradually increases to one. SF phase is characterized as ordered state, and MI phase is characterized as a disordered state. (c) Plot of complexity measures ($\Gamma_{\alpha\beta}$) as a function of V_0 . $\Gamma_{1/4,0}$, $\Gamma_{1,1}$, $\Gamma_{0,4}$ exhibit type I, type II, and type III complexity as discussed in the literature [27].

atoms in an optical lattice exhibit type II complexity during transition from SF phase to MI phase. The other complexity measures do not have any significance.

The most interesting is the distinct maxima in the LMC complexity measure which appears at $V_0 = 3.1$, which is very close to the point where order-disorder intersects. Thus, for the current system parameter, $V_0 = 3.1$ is the precursor point of entry to Mott phase and exit of SF phase. The calculation exhibits that LMC complexity is more efficient and detailed to find the entry-exit point, which is impossible to find from the monotonic increase in SIE.

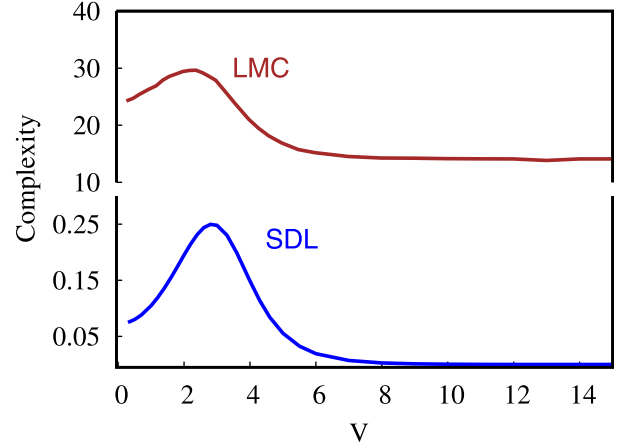


FIG. 4. Measures of complexity as a function of lattice depth (V_0). The upper graph is for LMC complexity measure and the lower one is for SDL ($\Gamma_{1,1}$) complexity measure. Initially, when the system is in SF phase, complexity has finite value. As V_0 increases, the system gets more and more fragmented, and its complexity also goes up, shows a maxima. Then, for large V_0 , when the system is in MI phase, it saturates to a fixed value. The saturation value is nearly zero for SDL measures and 14.6 for LMC measures. Both LMC and SDL ($\Gamma_{1,1}$) complexity exhibit nearly identical characteristics. The maxima in complexity measure indicates exit from SF phase and entry to MI phase.

To check the finite size effect, we pursue our numerical calculation in a large system with $N = 7$ particles in seven wells. The corresponding graphs showing the occupation in natural orbitals are presented in the Appendix. We observe how the initial state with occupation $|7, 0, 0, 0, 0, 0, 0\rangle$ gradually changes and then settle to $|1, 1, 1, 1, 1, 1, 1\rangle$ with increase in lattice depth V_0 which is a MI state. We have also calculated the LMC and SDL ($\Gamma_{1,1}$) complexity for this system and find no change in the behavior of complexity but amount of complexity increases as the system size increases. Thus, we can conclude that the qualitative measure of complexity is independent of the size of the system but quantitative measure is determined by the system size.

B. Dynamical measure of complexity for lattice depth quench

In this section, we discuss the dynamical measures of SIE and LMC complexity. The motivation of the study is three-fold. *First*: How does the system organize itself to optimize complexity during the quench? *Second*: How good is the dynamical measure of complexity to find out the timescale of dynamics? *Third*: To establish that dynamical measure of complexity is richer indicator than time dynamics of SIE. We monitor the time evolution of the natural orbitals, entropy production, and finally LMC complexity. In the dynamical evolution, the convergence is a serious issue and we need $M = 12$ orbitals for quench dynamics. We report long-time dynamics (up to $t = 300$) in all measured quantities. We initially prepare the system in SF phase with weak interaction strength $\lambda = 0.1$ in shallow lattice depth of $V_0 = 3.0$. We quench the system to MI phase by sudden increase in lattice depth to $V_0 = 10.0$. For dynamical analysis, we keep $N = 3$ particles in three wells. Of course, the dynamics of a large

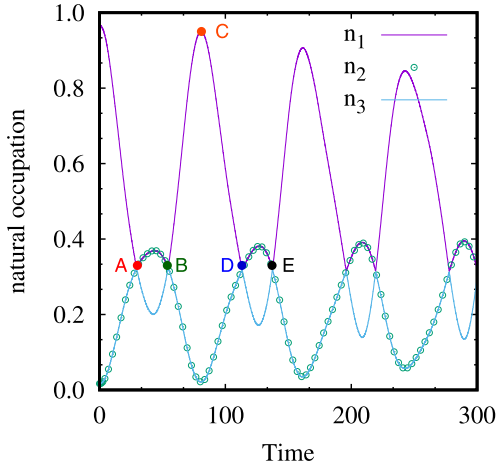


FIG. 5. Time evolution of natural occupation of $N = 3$ bosons in optical lattice as a function of time. The first three natural orbitals exhibit oscillation with time. Initially, when n_1 has a maximum and the other orbitals have a minimum, the state is known as the SF phase. At the crossing points of the first three orbitals, the system is in the MI phase with $n_1 \simeq n_2 \simeq n_3 \simeq \frac{1}{3}$. At point A ($t = 30.1$), three orbitals merge for the first time signifies first entry to MI phase. Point C ($t = 81.0$): when the system again achieves maximum contribution from the first orbital and negligible contribution from the other two. This is a SF phase. The other points at B ($t = 53.9$), D ($t = 113.1$), and E ($t = 137.2$) are explained in the text.

system can be handled. However, as convergence is a big issue in numerical simulation, we are unable to run the code with quite high numbers of natural orbitals. In Fig. 5, we plot the natural occupation in the first three orbitals as a function of time. At $t = 0.0$, only the first natural orbital contributes, which corresponds to SF phase. With increase in time, fragmentation occurs. We observe that at $t = 30.1$ (point A), the system is a fully fragmented MI state, the lowest three natural orbitals n_1, n_2, n_3 have close to 33% population. Between $t = 30.1$ to 53.9 (point B), n_1, n_2 overlap, n_3 becomes down. From the one-body correlation plot (not shown here), between $t = 30.1$ and 53.9, we find that the system exhibits only the diagonal correlation, which signifies the system is in MI phase. So, for this choice of parameter, MI state is retained in this interval. Then at $t = 81.0$ (point C), it enters to SF phase with maximum occupation only in the first orbital. At $t = 113.1$ (point D) it again enters the second MI phase and retained the MI phase until $t = 137.2$ (point E). The above scenario repeats with entry and exit in SF and MI phases. The timescale for different phases during the time evolution is presented in Table I for the first three cycles. We use integration time step equal to 0.1 in our numerical calculation. This basically simulates collapse-revival dynamics as observed in Greiner's experiment [44].

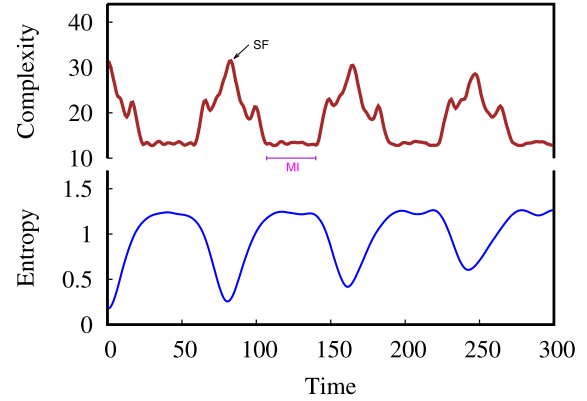


FIG. 6. Time evolution of LMC complexity and Shannon information entropy of $N = 3$ bosons in optical lattice as a function of time. Picks in LMC complexity (top) measures quantify the SF phase, and flat minima signify the holding time for the system in MI phase. The Shannon information entropy (bottom) exhibits maxima for MI phase and minima for SF phase. The MI state entry time can be determined with more accurately and efficiently using LMC complexity as there are distinct maxima or minima in LMC complexity.

The observations based on the timescale need further explanation. We calculate the time dependence in LMC complexity and Shannon information entropy and plot it in Fig. 6. We strictly follow the timescale of three cycles as presented in Table I. Our observations are as follows. (i) *For SF phase*: LMC complexity exhibits distinct maxima for all cycles. The same are represented by local minima in the entropy. (ii) *Mott state entry*: LMC complexity exhibits distinct minima. The broad peak in the entropy measure signifies the Mott state but the entry point is not distinct. (iii) *Mott phase*: LMC complexity shows distinct plateau in the same timescale as shown in Table I for all cycles. The corresponding SIE does not exhibit any clear plateau. In the first two cycles, there are broad, flat peaks but they gradually become deteriorated in the next cycle. Thus, it is not possible to precisely find the Mott holding time from the SIE measure. (iv) *MI state exit*: LMC measure shows sharp increase just after the plateau in the same timescale as in Table I. Corresponding SIE measure starts to fall but no distinct change can be claimed from the SIE measure. We may conclude that SIE exhibits qualitatively collapse-revival dynamics after the quench. However, due to *monotonic* oscillatory behavior, SIE is not able to predict any timescale of the dynamical evolution, whereas LMC complexity has *distinct* structure which clearly exhibits the same timescale of dynamics for all cycles which we have configured from the fragmentation. We conclude that the study of time evolution of SIE is not a very sensitive tool.

TABLE I. Superfluid to Mott-insulator phase transition time dynamics.

Period	SF state	Mott state entry	MI phase holding time	Mott state exit	SF state
First cycle	0.0	30.1	23.8	53.9	81.0
Second cycle	81.0	113.1	24.1	137.2	161.9
Third cycle	161.9	196.0	23.2	219.2	243.1

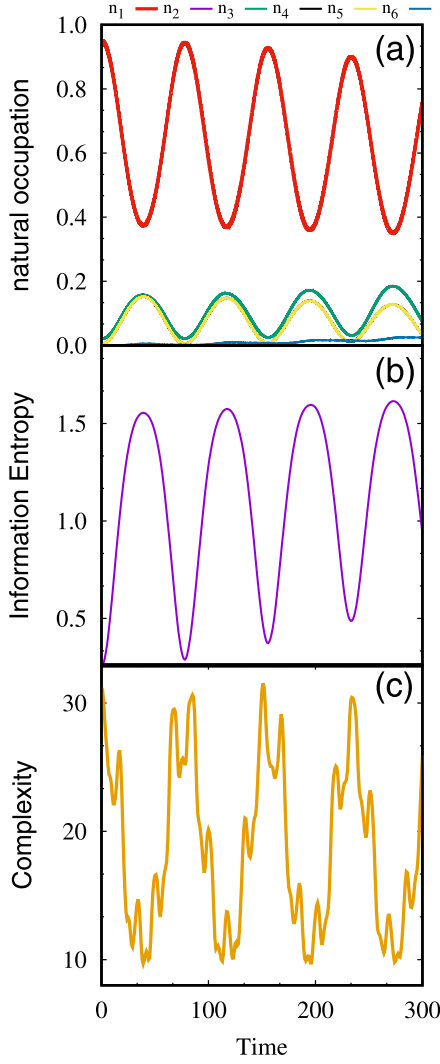


FIG. 7. Time dynamics of $N = 3$ bosons in $W = 5$ wells ($\nu < 1$). (a) Time evolution of natural orbitals as a function of time. The contributing orbitals exhibit oscillation but they do not merge together to form a MI phase. Here, n_2 and n_3 overlap and n_4 and n_5 overlap. Very small contribution from n_6 is noted. The contribution from n_i for $i > 6$ is insignificant and not shown here. (b) Plot of Shannon information entropy as a function of time. SIE oscillates in a same manner as in the case of $\nu = 1$. (c) Plot of LMC complexity as a function of time. Unlike the case of Fig. 6, here *no distinct* maxima, minima, or plateau region are observed. See text for further details.

In quench dynamics, a sudden increase in lattice depth means we are pumping energy into the system externally, and it will be distributed through the one-body term in the Hamiltonian. The system is able to distribute the extra energy between the interacting bosons and thus able to self-organize the external perturbation. But in the long-time dynamics, many excited states contribute in a complex manner. So it is very hard for the system to back in perfect SF phase, which is manifested by the slow decrease in height in the maxima of LMC measure.

However, to conclude whether LMC complexity measure can be taken as a rich universal indicator in finding the timescale of quench dynamics, we redo the simulation for

filling factor less than one. For $\nu < 1$, we choose $N = 3$ bosons in $W = 5$ wells, when entering a true Mott phase is not possible. Our goal is to find how the LMC complexity measure is able to distinguish imperfect Mott transition from a perfect Mott transition. For this case, we have calculated the natural occupation, SIE measure, and the LMC complexity and present our results in Fig. 7. From Fig. 7(a), it is clearly seen that complete fragmentation does not happen even in the long-time dynamics. We conclude that the Mott phases are not reached for this configuration. The corresponding SIE is plotted in Fig. 7(b). Entropy exhibits the similar kind of oscillation as observed in Fig. 6. One can now be misled as the maxima in the SIE correspond to Mott phase as discussed before ($\nu = 1$), although existence of Mott phase is already ruled out in the calculation of natural occupation in case of $\nu < 1$. The corresponding LMC complexity is plotted in Fig. 7(c). In the complexity measure, we do not find any distinct minima or maxima or plateau region which firmly confirm our conclusion from natural occupation. So, we can conclude that the SF to MI transition is not obtained for this chosen parameter. The very complex structure in the complexity additionally signifies that during time evolution, the system passes very complex phases which may be a fragmented SF phase or quasi-Mott phase. We conclude the same physics for $\nu > 1$, with same lattice depth quench.

V. CONCLUSION

“Statistical complexity” is one of the most circulating words in scientific research of physics, biology, mathematics, computer science, etc. Although there is no strictly followed definition of “what is complexity,” it is defined in many ways in the literature. From its vast application, it is found that LMC and SDL measures of complexity are well understood.

The measure of complexity has been extensively applied in different systems including atoms and molecules. Here we consider ultracold trapped atoms in the optical lattice which has been proved as a most challenging platform to study the many-body physics. Interacting bosons in the optical lattice exhibit different quantum phases like superfluid and Mott-insulator phases. The quantum phase transition has been experimentally studied as well as there are numerous theoretical calculations on the dynamical evolution. Although most of the calculations are based on mean-field level or utilizing Bose-Hubbard model, the strongly interacting bosons in shallow lattice deserve quantum many-body calculation. We report our results on a small ensemble of few particle systems utilizing the MCTDHB method which is exact by its construction and retains many-body correlation. We obtain many-body states which are the few-body analogy of different thermodynamic phases.

The main motivation of our work is how to consult the various quantum phases with the measure of SIE, order-disorder, and complexity. The intriguing question is how to justify complexity measure as the better descriptor than SIE in the quantum phase transition. Our present calculation is extensive, which includes both relaxed state and quenched state and covers different filling factors. For the relaxed state, the distinct maxima in the complexity measure clearly identify the crossover point from the SF to MI phase. Between the SF and Mott phases, corresponding SIE exhibits smooth increase and

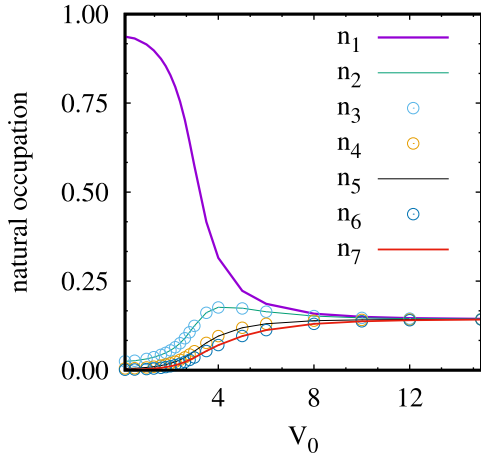


FIG. 8. Population of the first seven natural orbitals as a function of lattice depth (V_0) for $N = 7$ bosons in seven-well one-dimensional optical lattice. As V_0 increases, the occupation in the first orbital starts to decrease while the other six orbitals start to contribute. At $V_0 = 12.0$, the state becomes sevenfold fragmented ($n_1 \simeq n_2 \simeq n_3 \simeq n_4 \simeq n_5 \simeq n_6 \simeq n_7 \simeq \frac{1}{7}$).

absolutely fails to detect the exit of SF phase and entry to MI phase. The results for dynamics is more rich and informative. Additionally, we get the full timescale of dynamics in different cycles from the complexity measures. The distinct structure in complexity makes it richer than the monotonic behavior of SIE. For incommensurate filling factor, when the SF \rightarrow MI transition is incomplete, we observe that the SIE may even lead to conclude wrong physics. The dynamical structural difference in complexity provides a clear signature of such incomplete phase transition. This elaborate calculation leads to conclude that complexity measure is not only richer, but it can be taken as a “figure of merit” to identify the transition point.

ACKNOWLEDGMENTS

R. Roy acknowledges the University Grant Commission (UGC) India for the financial support as a senior research fellow. The authors are grateful to K. D. Sen for his reading of the manuscript and valuable comments. The authors gratefully acknowledge the invaluable feedback and suggestions of the anonymous reviewers. N.D.C. acknowledges support from university research project grant (Grant No. GCU/RCC/2021-22/20-32/508).

APPENDIX: NATURAL OCCUPATION AND COMPLEXITY FOR $N = 7$ BOSONS IN SEVEN WELLS

In this Appendix, we report the relaxed state calculation for seven bosons in seven-well optical lattice. Although we keep the commensurate filling factor, i.e., $\nu = \frac{N}{W} = 1$, however, as the number of particles are now increased, a greater number of natural orbitals began to participate. For convergence, we

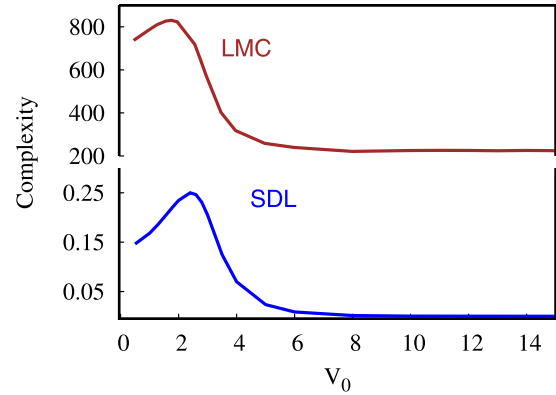


FIG. 9. Measures of complexity as a function of lattice depth (V_0) for $N = 7$ bosons in seven-well one-dimensional optical lattice. The upper graph is for LMC complexity measure and the lower one is for SDL complexity measure. Initially, when the system is in SF phase, complexity has finite value. As V_0 increases, the system gets fragmented and both the complexity increases, shows maxima, and then saturates to a finite value for large V_0 , when the system is in MI phase. Both LMC and SDL complexity exhibit nearly identical characteristics.

keep $M = 21$ orbitals in our simulation. In Fig. 8, we plot the natural occupation in the first seven orbitals. The contributions of the remaining orbitals are negligible. For extremely small lattice depth, the first orbital is nearly completely occupied, whereas the other orbitals have little occupancy. The single orbital mean-field state provides a good approximation for the many-body wave function as $N = |7, 0, 0, 0, 0, 0, 0\rangle$. We can call this as SF phase. Participation from the remaining six orbitals begins to contribute as lattice depth increases. At $V_0 = 12.0$, contributions from the seven orbitals saturate to 14.2% and we get sevenfold fragmented MI phase. In Fig. 9, we plot the LMC and SDL measures of complexity. As discussed in the main text, $\Gamma_{1,1}$ is the most deterministic measure of SDL complexity for our system. Here we compare only $\Gamma_{1,1}$ with LMC complexity. As higher number of orbitals are now participating, complexity will be more in case of LMC measure as expected. When V_0 is small, state is superfluid, and complexity has a finite value. Complexity builds up gradually and reaches a maximum as lattice depth increases. This peak is reached when the system is in a mixed state of SF and MI. When the system is perfectly in MI state, complexity saturates. The same type of behavior is exhibited by both SDL and LMC complexity. Both the SDL and LMC complexity have same kind of nature for $N = 3$ and 7 particles. In LMC measure, complexity is more for $N = 7$ compared to $N = 3$ case. This is quite obvious as the number of particles of a system increase, the system will spread more in the Hilbert space. Thus, for bosons in an optical lattice, $\Gamma_{1,1}$ is a reasonable choice for measuring system complexity, and the nature of complexity is independent of the size of the Hilbert space.

[1] Y. Huang, *IEEE Trans. Inf. Theory* **59**, 6774 (2013).
 [2] J. Angulo and J. Antolín, *J. Chem. Phys.* **128**, 164109 (2008).

[3] I. V. Toranzo, P. Sánchez-Moreno, Ł. Rudnicki, and J. S. Dehesa, *Entropy* **19**, 16 (2016).

- [4] A. Guerrero, P. Sánchez-Moreno, and J. S. Dehesa, *Phys. Rev. A* **84**, 042105 (2011).
- [5] J. Angulo, J. Antolín, and K. Sen, *Phys. Lett. A* **372**, 670 (2008).
- [6] N. Sobrino-Coll, D. Puertas-Centeno, I. Toranzo, and J. Dehesa, *J. Stat. Mech.* (2017) 083102.
- [7] I. Prigogine and G. Nicolis, in *Self-Organisation in Nonequilibrium Systems: Towards A Dynamics of Complexity* (Springer, Dordrecht, 1985), pp. 3–12.
- [8] B. Huberman and T. Hogg, *Phys. D (Amsterdam)* **22**, 376 (1986).
- [9] S. A. Astashkevich, *Phys. Lett. A* **383**, 2854 (2019).
- [10] S. Massen and C. Panos, *Phys. Lett. A* **246**, 530 (1998).
- [11] S. R. Gadre, S. B. Sears, S. J. Chakravorty, and R. D. Bendale, *Phys. Rev. A* **32**, 2602 (1985).
- [12] S. R. Gadre and R. D. Bendale, *Phys. Rev. A* **36**, 1932 (1987).
- [13] R. J. Yáñez, W. Van Assche, and J. S. Dehesa, *Phys. Rev. A* **50**, 3065 (1994).
- [14] I. Białyński-Birula and J. Mycielski, *Commun. Math. Phys.* **44**, 129 (1975).
- [15] K. C. Chatzisavvas, C. C. Moustakidis, and C. Panos, *J. Chem. Phys.* **123**, 174111 (2005).
- [16] C. Adami and N. Cerf, *Phys. D (Amsterdam)* **137**, 62 (2000).
- [17] J. R. Sánchez and R. López-Ruiz, *Phys. A (Amsterdam)* **355**, 633 (2005).
- [18] X. Calbet and R. López-Ruiz, *Phys. Rev. E* **63**, 066116 (2001).
- [19] M. Escalona-morán, M. G. Cosenza, R. López-Ruiz, and P. García, *Int. J. Bifurcation Chaos* **20**, 1723 (2010).
- [20] D. P. Feldman and J. P. Crutchfield, *Phys. Lett. A* **238**, 244 (1998).
- [21] M. Martin, A. Plastino, and O. Rosso, *Phys. Lett. A* **311**, 126 (2003).
- [22] E. H. Lieb, *Rev. Mod. Phys.* **48**, 553 (1976).
- [23] C. Panos, K. Chatzisavvas, C. Moustakidis, and E. Kyrkou, *Phys. Lett. A* **363**, 78 (2007).
- [24] R. G. Catalán, J. Garay, and R. López-Ruiz, *Phys. Rev. E* **66**, 011102 (2002).
- [25] K. D. Sen, *Statistical Complexity: Applications in Electronic Structure* (Springer, New York, 2011).
- [26] R. López-Ruiz, *Biophys. Chem.* **115**, 215 (2005).
- [27] J. S. Shiner, M. Davison, and P. T. Landsberg, *Phys. Rev. E* **59**, 1459 (1999).
- [28] R. López-Ruiz, H. Mancini, and X. Calbet, *Phys. Lett. A* **209**, 321 (1995).
- [29] S. J. C. Salazar, H. G. Laguna, and R. P. Sagar, *Eur. Phys. J. Plus* **137**, 19 (2022).
- [30] C. Martínez-Flores, *Phys. Lett. A* **386**, 126988 (2021).
- [31] S. J. C. Salazar, H. G. Laguna, and R. P. Sagar, *Quantum Rep.* **2**, 560 (2020).
- [32] S. J. C. Salazar, H. G. Laguna, and R. P. Sagar, *Phys. Rev. A* **101**, 042105 (2020).
- [33] R. K. Kumar, B. Chakrabarti, and A. Gammal, *J. Low Temp. Phys.* **194**, 14 (2019).
- [34] C. Moustakidis and C. Panos, *Phys. Lett. A* **382**, 1563 (2018).
- [35] G. Ferri, F. Pennini, and A. Plastino, *Phys. A (Amsterdam)* **545**, 123648 (2020).
- [36] R. Roy, A. Gammal, M. C. Tsatsos, B. Chatterjee, B. Chakrabarti, and A. U. J. Lode, *Phys. Rev. A* **97**, 043625 (2018).
- [37] M. Greiner, O. Mandel, T. Esslinger, T. W. Hänsch, and I. Bloch, *Nature (London)* **415**, 39 (2002).
- [38] I. Danshita and A. Polkovnikov, *Phys. Rev. A* **84**, 063637 (2011).
- [39] M. Capello, F. Becca, M. Fabrizio, and S. Sorella, *Phys. Rev. Lett.* **99**, 056402 (2007).
- [40] B. Chatterjee and A. U. J. Lode, *Phys. Rev. A* **98**, 053624 (2018).
- [41] B. Chatterjee, M. C. Tsatsos, and A. U. J. Lode, *New J. Phys.* **21**, 033030 (2019).
- [42] R. Lin, L. Papariello, P. Mognini, R. Chitra, and A. U. J. Lode, *Phys. Rev. A* **100**, 013611 (2019).
- [43] S. Bera, R. Roy, A. Gammal, B. Chakrabarti, and B. Chatterjee, *J. Phys. B: At. Mol. Opt. Phys.* **52**, 215303 (2019).
- [44] M. Greiner, O. Mandel, T. W. Hänsch, and I. Bloch, *Nature (London)* **419**, 51 (2002).
- [45] R. Lin, P. Mognini, L. Papariello, M. C. Tsatsos, C. Lévêque, S. E. Weiner, E. Fasshauer, R. Chitra, and A. U. J. Lode, *Quantum Sci. Technol.* **5**, 024004 (2020).
- [46] A. U. J. Lode, *Phys. Rev. A* **93**, 063601 (2016).
- [47] A. U. J. Lode, C. Lévêque, L. B. Madsen, A. I. Streltsov, and O. E. Alon, *Rev. Mod. Phys.* **92**, 011001 (2020).
- [48] O. E. Alon, A. I. Streltsov, and L. S. Cederbaum, *J. Chem. Phys.* **127**, 154103 (2007).
- [49] O. E. Alon, A. I. Streltsov, and L. S. Cederbaum, *Phys. Rev. A* **77**, 033613 (2008).
- [50] A. U. J. Lode, K. Sakmann, O. E. Alon, L. S. Cederbaum, and A. I. Streltsov, *Phys. Rev. A* **86**, 063606 (2012).
- [51] R. Roy, C. Lévêque, A. U. J. Lode, A. Gammal, and B. Chakrabarti, *Quantum Rep.* **1**, 304 (2019).
- [52] S. Bera, R. Roy, and B. Chakrabarti, in *Proceedings of the National Conference on Frontiers in Modern Physics (NCFMP-2018)*, AIP Conference Proceedings (AIP, Melville, NY, 2019), Vol. 2072, p. 020011.
- [53] R. Roy, B. Chakrabarti, and A. Trombettoni, *Eur. Phys. J. D* **76**, 24 (2022).
- [54] R. Lin, C. Georges, J. Klinder, P. Mognini, M. Büttner, A. U. J. Lode, R. Chitra, A. Hemmerich, and H. Keßler, *SciPost Phys.* **11**, 030 (2021).
- [55] J. H. V. Nguyen, M. C. Tsatsos, D. Luo, A. U. J. Lode, G. D. Telles, V. S. Bagnato, and R. G. Hulet, *Phys. Rev. X* **9**, 011052 (2019).
- [56] A. U. J. Lode, B. Chakrabarti, and V. K. B. Kota, *Phys. Rev. A* **92**, 033622 (2015).
- [57] S. Kvaal, *Mol. Phys.* **111**, 1100 (2013).
- [58] P. Kramer and M. Saraceno, *Geometry of the Time-Dependent Variational Principle in Quantum Mechanics* (Springer, Berlin, 1981).
- [59] A. McLachlan, *Mol. Phys.* **8**, 39 (1964).
- [60] L. Cao, V. Bolsinger, S. I. Mistakidis, G. M. Koutentakis, S. Krönke, J. M. Schurer, and P. Schmelcher, *J. Chem. Phys.* **147**, 044106 (2017).
- [61] A. I. Streltsov, O. E. Alon, and L. S. Cederbaum, *Phys. Rev. Lett.* **99**, 030402 (2007).
- [62] E. Fasshauer and A. U. J. Lode, *Phys. Rev. A* **93**, 033635 (2016).
- [63] A. U. J. Lode and C. Bruder, *Phys. Rev. A* **94**, 013616 (2016).
- [64] J. P. Crutchfield, D. P. Feldman, and C. R. Shalizi, *Phys. Rev. E* **62**, 2996 (2000).
- [65] R. J. Glauber, *Phys. Rev.* **130**, 2529 (1963).

- [66] K. Sakmann, A. I. Streltsov, O. E. Alon, and L. S. Cederbaum, *Phys. Rev. A* **78**, 023615 (2008).
- [67] T. Langen, S. Erne, R. Geiger, B. Rauer, T. Schweigler, M. Kuhnert, W. Rohringer, I. E. Mazets, T. Gasenzer, and J. Schmiedmayer, *Science* **348**, 207 (2015).
- [68] S. S. Hodgman, R. G. Dall, A. G. Manning, K. G. H. Baldwin, and A. G. Truscott, *Science* **331**, 1046 (2011).
- [69] T. Schweigler, V. Kasper, S. Erne, I. Mazets, B. Rauer, F. Cataldini, T. Langen, T. Gasenzer, J. Berges, and J. Schmiedmayer, *Nature (London)* **545**, 323 (2017).
- [70] R. G. Dall, A. G. Manning, S. S. Hodgman, W. RuGway, K. V. Kheruntsyan, and A. G. Truscott, *Nat. Phys.* **9**, 341 (2013).
- [71] J. C. Angulo and S. López-Rosa, *Entropy* **24**, 233 (2022).